

# Supporting Information

## **Polymer-supported Zn-containing imidazolium salt ionic liquids as sustainable catalysts for the cycloaddition of CO<sub>2</sub>: A kinetic study and response surface methodology**

*Dongwoo Kim, Hoon Ji, Moon Young Hur, Wonjoo Lee, Tea Soon Kim, and Deug-Hee Cho\**

Advanced Industrial Chemistry Research Center, Korea Research Institute of Chemical  
Technology, 45, Jongga-ro, Jung-gu, Ulsan 44412, Republic of Korea

### **\* Corresponding author**

E-mail address: dhcho@kriict.re.kr

Tel.: +82 52 241 6040; fax: +82 52 241 6049.

**The number of pages (including cover page): 19**

**The number of figures: 11 (Figure S1 – S11)**

**The number of tables: 6 (Table S1 – S6)**

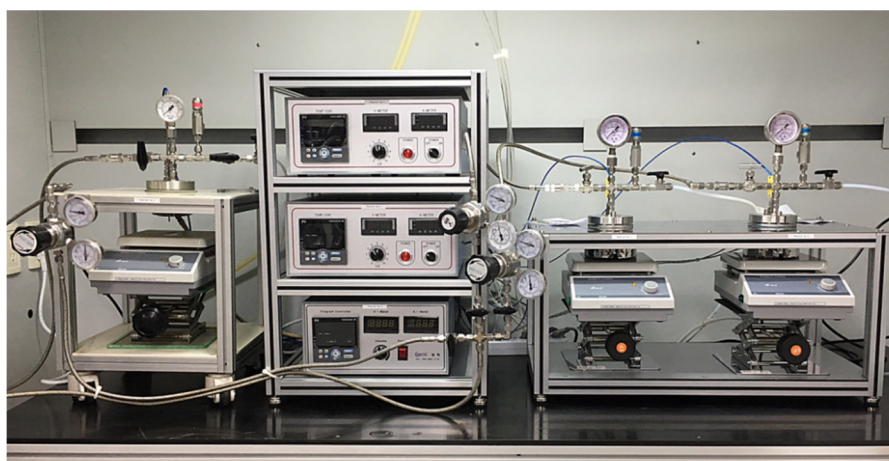
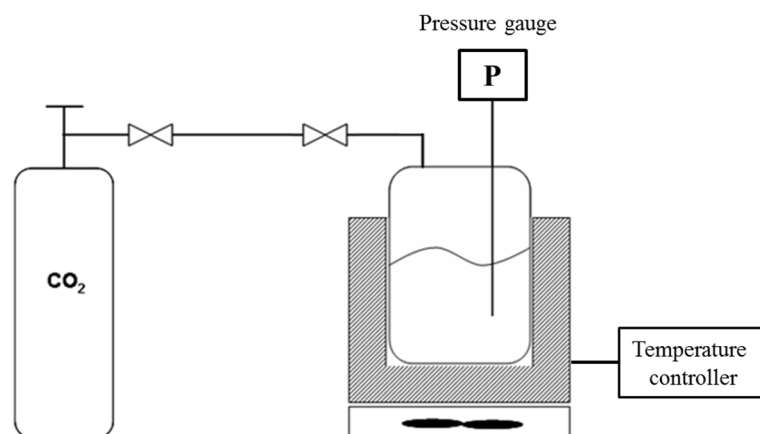


Figure S1. Apparatus for the cycloaddition of  $\text{CO}_2$  and epoxide

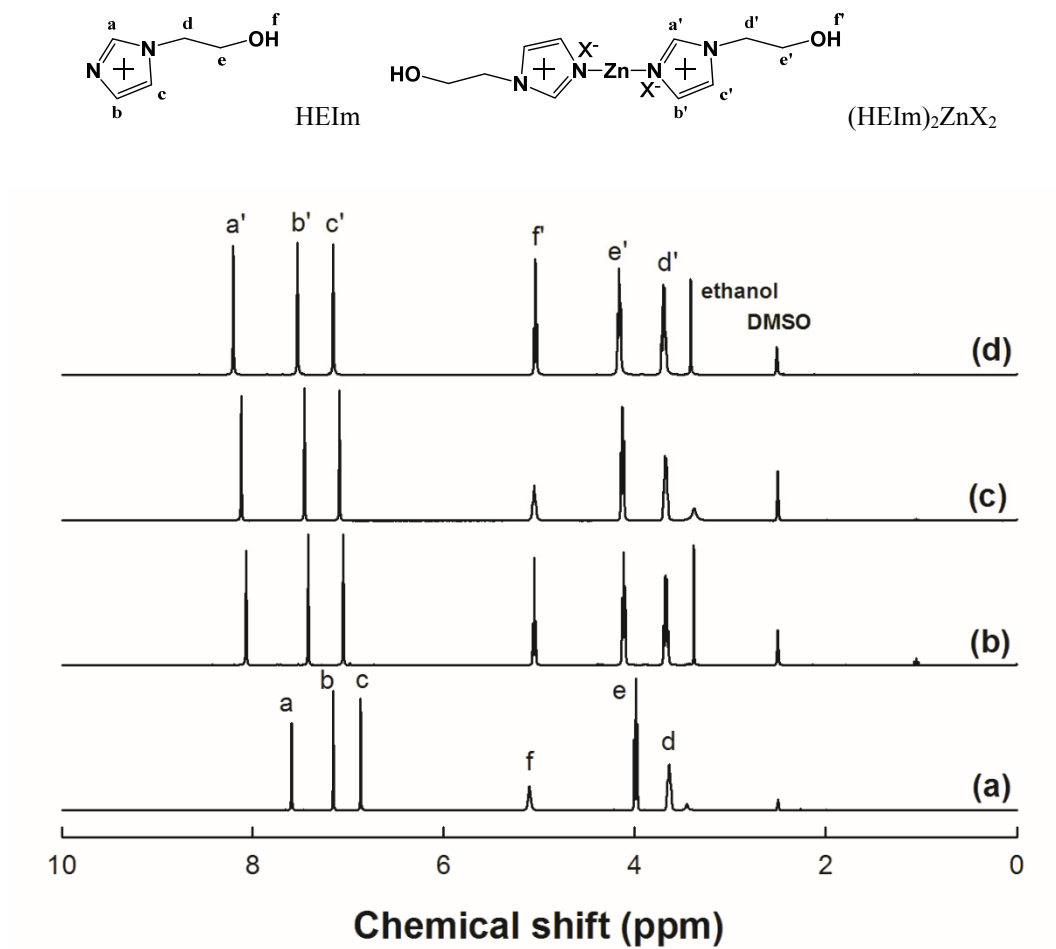


Figure S2.  $^1\text{H}$ -NMR Spectra of (a) HEIm, (b) (HEIm) $_2\text{ZnCl}_2$ , (c) (HEIm) $_2\text{ZnBr}_2$ , and (d) (HEIm) $_2\text{ZnI}_2$ .

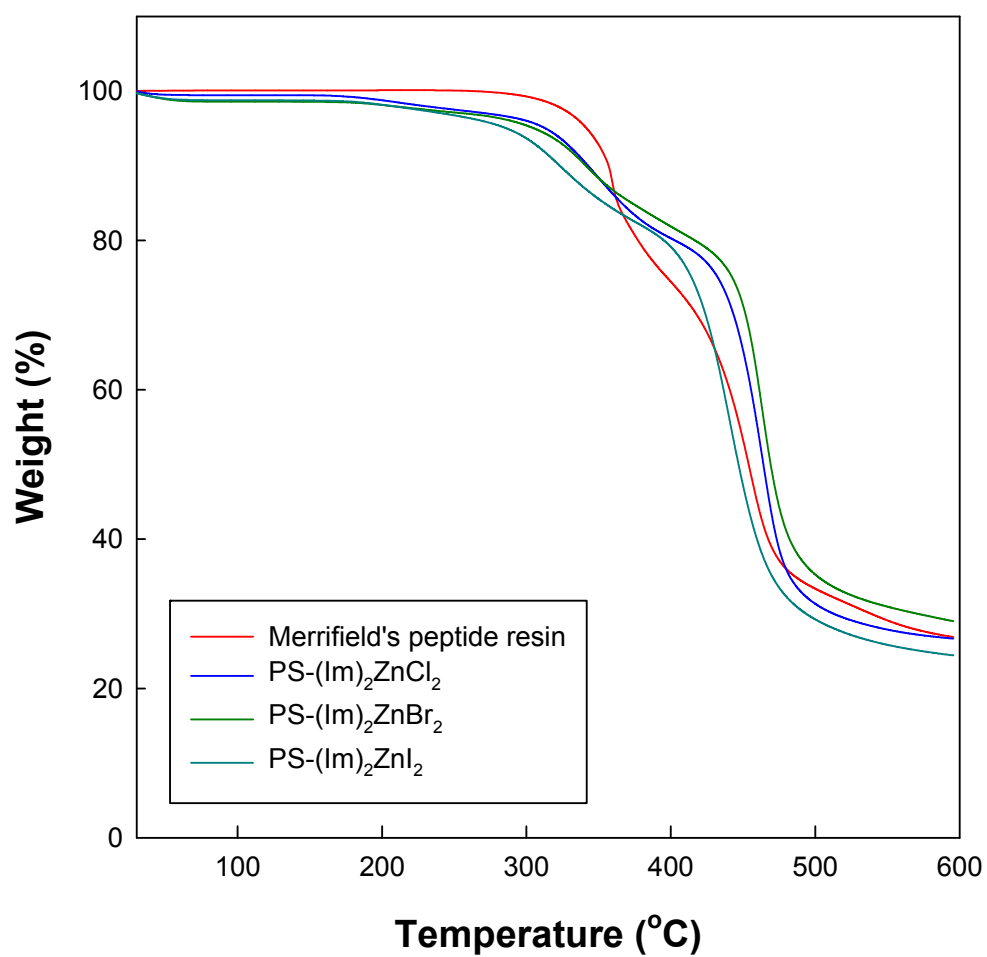


Figure S3. TGA results of Merrifield's peptide resin and PS-(Im)<sub>2</sub>ZnX<sub>2</sub>.

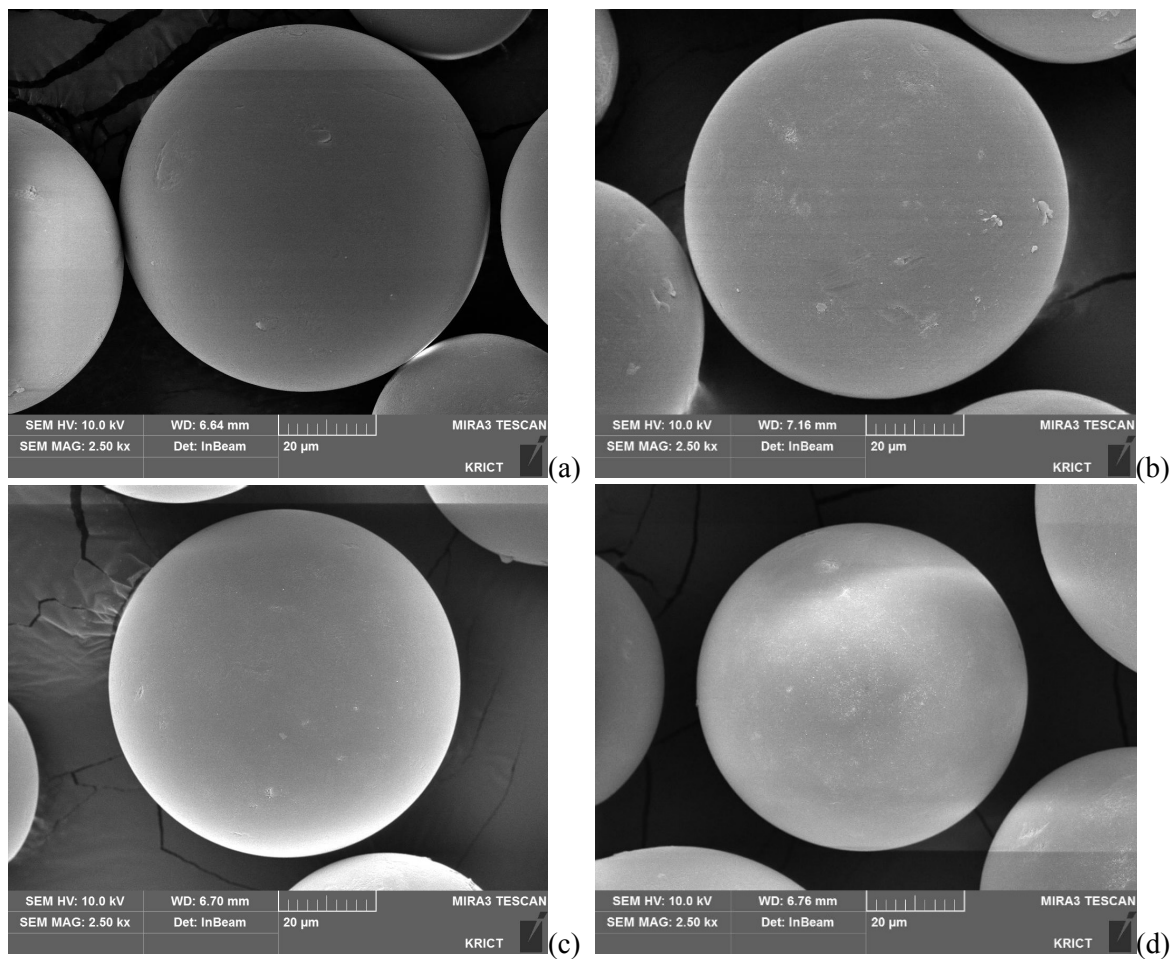


Figure S4. SEM image of (a) Merrifield's peptide resin, (b) PS-(Im)<sub>2</sub>ZnCl<sub>2</sub>, (c) PS-(Im)<sub>2</sub>ZnBr<sub>2</sub> and (d) PS-(Im)<sub>2</sub>ZnI<sub>2</sub>.

Table S1. The effect of reaction time at different temperatures and 10 bar CO<sub>2</sub> pressure in the batch and semi-batch systems.

Entry	Reaction time (h)	Temperature (°C)	batch system		semi-batch system	
			Conversion of PO (%)	Selectivity to PC (%)	Conversion of PO (%)	Selectivity to PC (%)
1	1	40	8.3	> 99	10.3	> 99
2	2		14.2	> 99	17.7	> 99
3	3		18.1	> 99	24.4	> 99
4	1	50	17.2	> 99	30.2	> 99
5	2		29.3	> 99	45.0	> 99
6	3		38.2	> 99	54.9	> 99
7	1	60	31.3	> 99	52.1	> 99
8	2		48.5	> 99	72.5	> 99
9	3		60.2	> 99	80.6	> 99

Reaction conditions: 50 mmol PO, 0.2 g of PS-(Im)<sub>2</sub>ZnI<sub>2</sub>.

**Statistical analysis of RSM and optimization of reaction conditions.** The response surface methodology (RSM) is a powerful statistical tool for the optimization of numerous experimental variables with a minimum number of trials. The Box–Behnken design (BBD) was employed to obtain optimized reaction conditions with a high yield of PC under a mild reaction environment for batch and semi-batch systems. The important variables used were the temperature ( $X_1$ ), the  $\text{CO}_2$  pressure ( $X_2$ ), and reaction time ( $X_3$ ). These variables were coded to three levels, and the experimental range and the central points for each factor are shown in Table S2. This quadratic equation was used to predict the optimum values and to elucidate the interactions between the variables. The equation is expressed as Eq. (S1):

$$Y = \lambda_0 + \sum_{i=1}^3 \lambda_i X_i + \sum_{i=1}^3 \lambda_{ii} X_i^2 + \sum_{i=1}^2 \sum_{j=i+1}^3 \lambda_{ij} X_i X_j \quad (\text{S1})$$

Where,  $\lambda_0$  (constant term),  $\lambda_i$  (linear effect term),  $\lambda_{ii}$  (squared effect term), and  $\lambda_{ij}$  (interaction effect term) are regression coefficients, and Y is the predicted response value (yield of PC). All data were analyzed using the Expert Design 11 software package, and the significant second-order coefficients were selected by regression analysis with backward elimination from the analysis of variance (ANOVA).

Table S2. Coded levels for independent factors used in the experimental design.

variable	Symbol	Coded levels		
		-1	0	1
Temperature ( $^{\circ}\text{C}$ )	$X_1$	30	50	70
Pressure (bar)	$X_2$	5	10	15
Reaction time (h)	$X_3$	4	12	20

Here, because the PS-(Im)<sub>2</sub>ZnI<sub>2</sub> catalyst can be considered an efficient catalyst for the cycloaddition of PO to CO<sub>2</sub>, the BBD was applied to model the yield of PC from CO<sub>2</sub> using PS-(Im)<sub>2</sub>ZnCl<sub>2</sub> catalysis with three reaction parameters: the temperature (X<sub>1</sub>), CO<sub>2</sub> pressure (X<sub>2</sub>), and reaction time (X<sub>3</sub>). BBD center-united designs were employed for the experiments, and the corresponding response values are shown in Table S3 for the batch and semi-batch systems, respectively. Based on BBD, 15 runs with three parameters were used to derive an objective function for the yield of PC. Table S4 shows the analysis of variance (ANOVA) of the responses for the batch and semi-batch systems, respectively. The correlation coefficient ( $R^2$ ) for the yield of PC is 0.9965 (batch system) and 0.9977 (semi-batch system), which demonstrates that the theoretical values are in good accordance with the experimental values. The polynomial models for the yield of PC (Y) obtained from the experimental design are as follows Eq. (S2) (Y<sub>1</sub>, batch system) and Eq. (S3) (Y<sub>2</sub>, semi-batch system).

$$Y_1 = 73.28 + 23.70 \cdot X_1 + 11.63 \cdot X_2 + 15.48 \cdot X_3 + 0.58 \cdot X_1 \cdot X_2 - 9.50 \cdot X_1 \cdot X_3 + 8.86 \cdot X_2 \cdot X_3 - 1.56 \cdot X_1^2 - 8.46 \cdot X_2^2 - 4.58 \cdot X_3^2 \quad (S2)$$

$$Y_2 = 86.03 + 27.45 \cdot X_1 + 3.36 \cdot X_2 + 11.56 \cdot X_3 - 1.67 \cdot X_1 \cdot X_2 - 9.53 \cdot X_1 \cdot X_3 - 2.50 \cdot X_2 \cdot X_3 - 13.69 \cdot X_1^2 - 0.267 \cdot X_2^2 - 1.97 \cdot X_3^2 \quad (S3)$$

The p-value can be used as an index to check the significance of each coefficient and the terms with smaller p-value (less than 0.05) are more significant. In case of batch system, the linear terms of X<sub>1</sub>, X<sub>2</sub> and X<sub>3</sub> are significant, whereas the linear terms of X<sub>1</sub> and X<sub>3</sub>, and quadratic term of X<sub>1</sub><sup>2</sup> are significant for semi-batch system (Table S4). The temperature parameter (X<sub>1</sub>) has the major linear effect on yield of PC for the both systems. However, the CO<sub>2</sub> pressure parameter (X<sub>2</sub>) affects the batch system only. Contour plots are commonly used to evaluate the relationships between parameters and to predict the result under the given



conditions. The RSM profiles for the three parameters were constructed using the above-mentioned model for the yield of PC, and they are plotted as a function of two factors. The remaining parameter was maintained at a constant center level (Figure S5). As shown in Figure S5(a, c, and e), the high levels of all three parameters show a maximum yield of PC for the batch system. On the other hand, a high yield of PC is achieved above level 0.5 of temperature and longer reaction times at any level of CO<sub>2</sub> pressure (Figure S5(b, d, and f)) for the semi-batch system. The optimal reaction conditions under a moderate environment for the batch and semi-batch system are summarized in Table S6. The optimized reaction conditions for the batch system are 60 °C (level 0.5) temperature, 15 bar (level 1) CO<sub>2</sub> pressure, and 17.6 h (level 0.7) reaction time, and the maximum yield of PC for the semi-batch system was obtained at 60 °C (level 0.5) at 15 bar (level 1) after 12.8 h (level 0.1). To validate the models, three independent experiments for each batch and semi-batch systems were carried out under the optimized conditions (Table S6). The average experimental yields of PO were  $99.32 \pm 0.03\%$  for the batch system and  $99.91 \pm 0.03\%$  for the semi-batch system, which are values close to the predicted yields. Thus, RSM with an appropriate experimental design is an effective tool for optimizing the cycloaddition of CO<sub>2</sub> using the PS-(Im)<sub>2</sub>ZnI<sub>2</sub> catalyst for both batch and semi-batch systems.

Table S3. Experimental design and results of the RSD for batch and semi-batch system.

No.	X <sub>1</sub>	X <sub>2</sub>	X <sub>3</sub>	batch system	semi-batch system
				Yield of PC (%)	
1	-1	-1	0	29.1	41.2
2	1	-1	0	76.4	98.7
3	-1	1	0	48.9	48.8
4	1	1	0	98.6	99.6
5	-1	0	-1	17.6	22.3
6	1	0	-1	82.9	97.0
7	-1	0	1	70.4	62.8
8	1	0	1	97.7	99.4
9	0	-1	-1	42.3	64.3
10	0	1	-1	50.1	78.5
11	0	-1	1	52.7	94.1
12	0	1	1	95.9	98.3
13	0	0	0	72.7	86.0
14	0	0	0	72.6	86.0
15	0	0	0	71.5	86.1

Table S4. Coefficients of the model and ANOVA for batch and semi-batch system.

Term	batch system		semi-batch system	
	Coefficient	P-value (Prob. > F)	Coefficient	P-value (Prob. > F)
Intercept	73.28	< 0.0001	86.03	< 0.0001
X <sub>1</sub>	23.70	< 0.0001	27.45	< 0.0001
X <sub>2</sub>	11.63	< 0.0001	3.36	0.0046
X <sub>3</sub>	15.48	< 0.0001	11.56	< 0.0001
X <sub>1</sub> ·X <sub>2</sub>	0.58	0.6432	-1.67	0.1463
X <sub>1</sub> ·X <sub>3</sub>	-9.50	0.0006	-9.53	0.0002
X <sub>2</sub> ·X <sub>3</sub>	8.86	0.0008	-2.50	0.0503
X <sub>1</sub> <sup>2</sup>	-1.56	0.4419	-13.69	< 0.0001
X <sub>2</sub> <sup>2</sup>	-8.46	0.0015	-0.267	0.8031
X <sub>3</sub> <sup>2</sup>	-4.58	0.0240	-1.97	0.1102
R <sup>2</sup>	0.9965		0.9977	

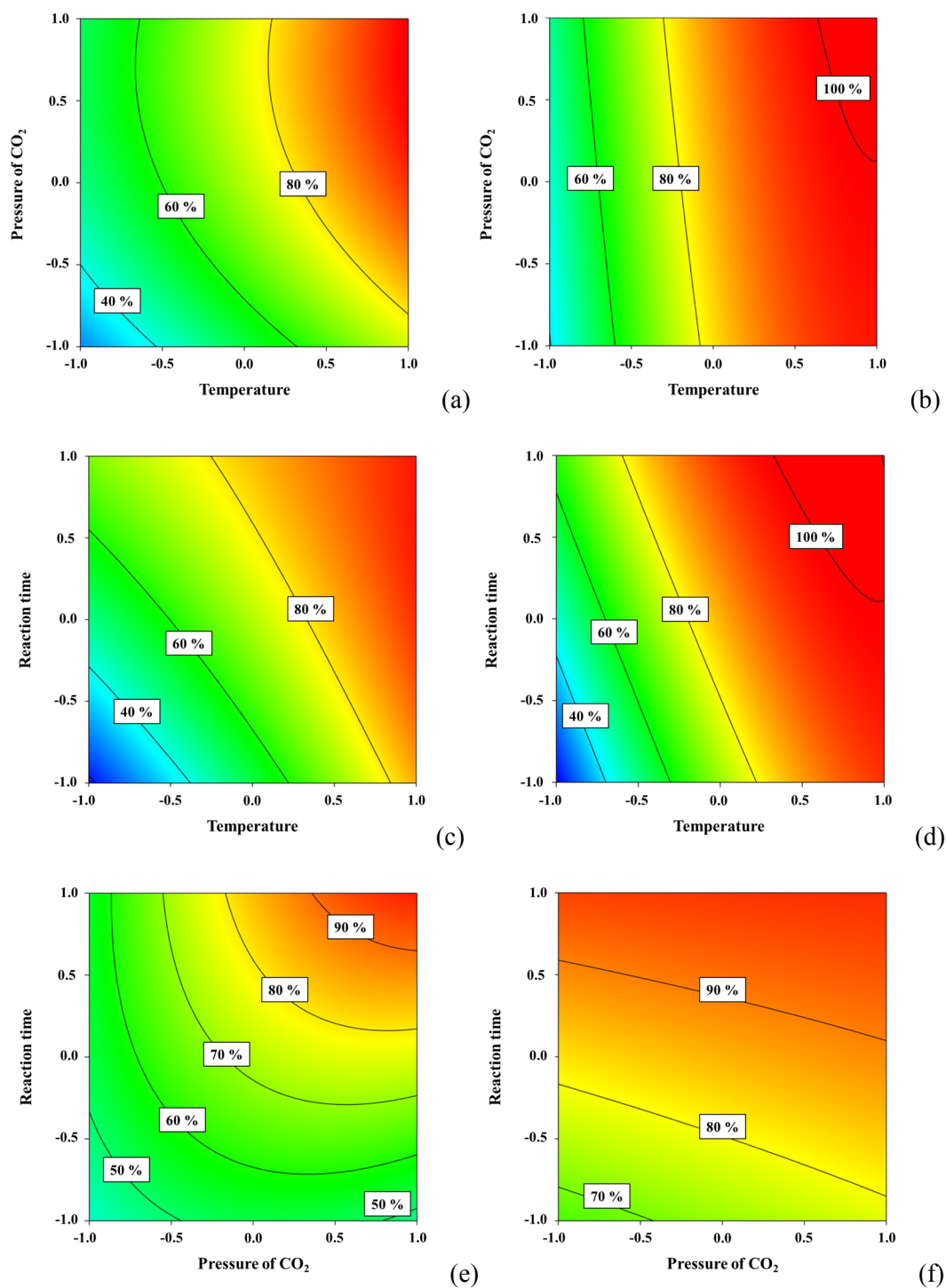


Figure S5. Contour of the yield of PC for batch (left) and semi-batch (right) system; (a, b) pressure of CO<sub>2</sub> and temperature, (c, d) reaction time and temperature, (e, f) reaction time and pressure of CO<sub>2</sub>. The remaining parameter was held at its mean level.

Table S6. Predicted and experimental results under the optimum reaction conditions for batch and semi-batch system.

System	Temperature (°C)	Pressure of CO <sub>2</sub> (bar)	Reaction time (h)	Yield of PC (%)	
				Predicted	Experimental
batch	60 (0.5)	15 (1)	17.6 (0.7)	99.67	99.32 ± 0.03%
semi-batch	60 (0.5)	15 (1)	12.8 (0.1)	99.69	99.91 ± 0.03%

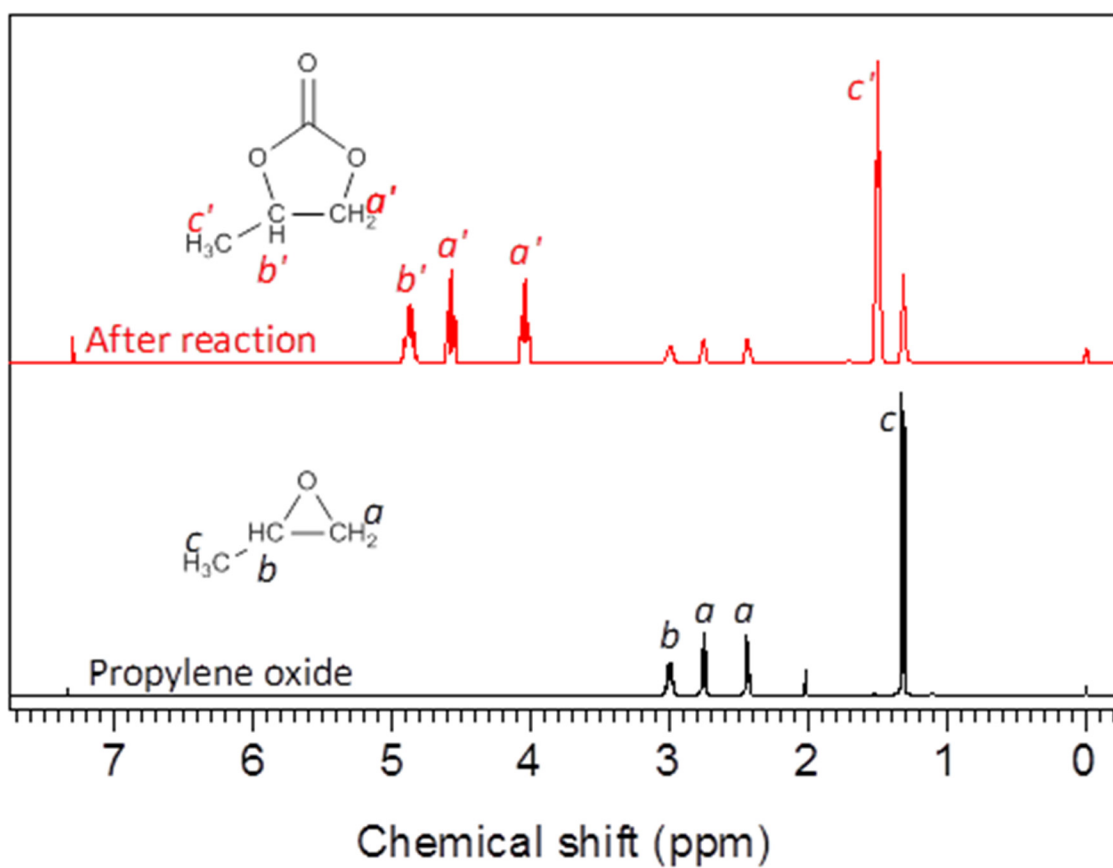


Figure S6. <sup>1</sup>H-NMR spectra of 2-methyloxirane (propylene oxide) and 4-methyl-1,3-dioxolan-2-one (propylene carbonate) in CDCl<sub>3</sub>.

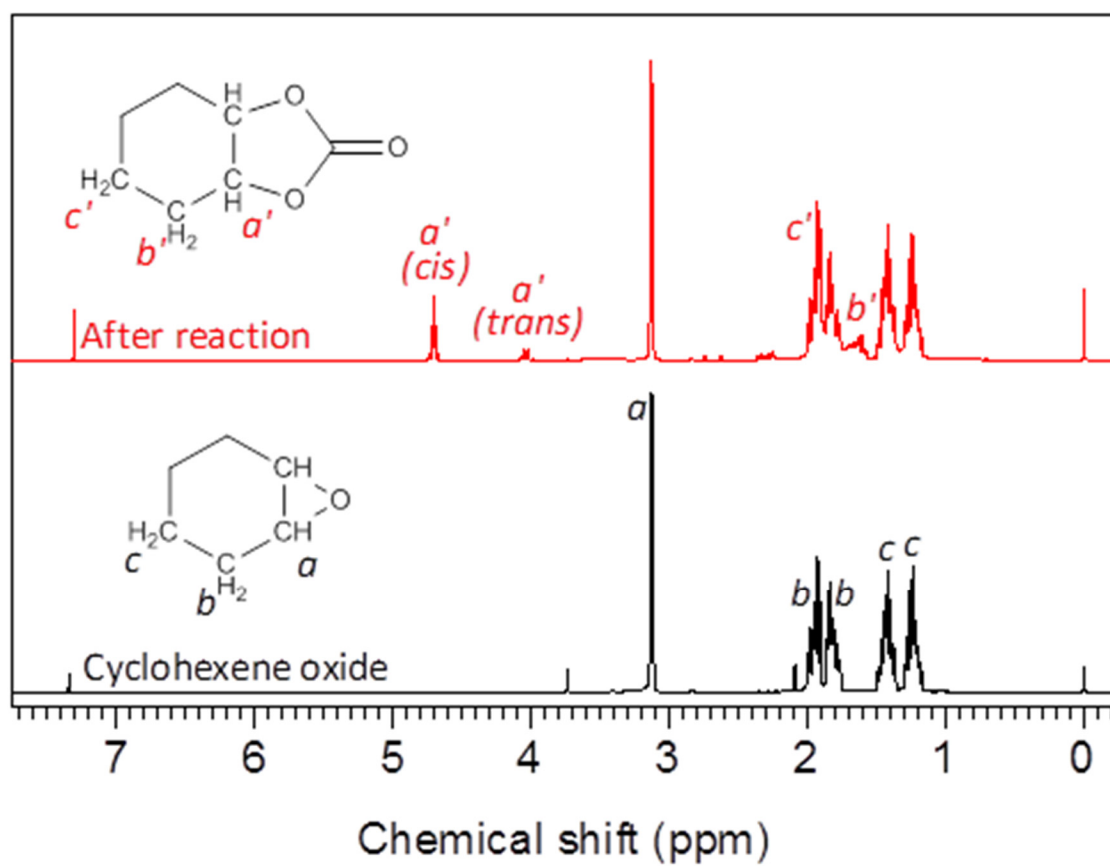


Figure S7.  $^1\text{H}$ -NMR spectra of 7-oxabicyclo[4.1.0]heptane (cyclohexene oxide) and hexahydrobenzo[*d*][1,3]dioxol-2-one (cyclohexene carbonate) in  $\text{CDCl}_3$ .

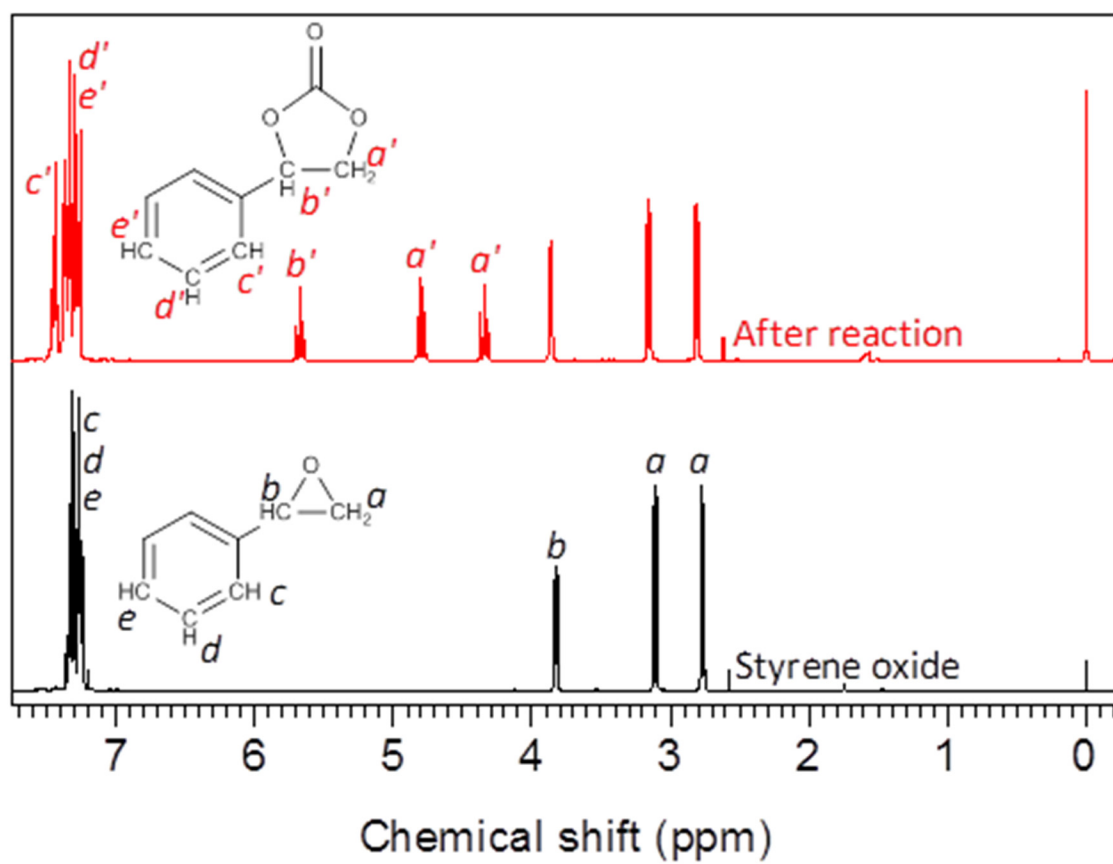


Figure S8. <sup>1</sup>H-NMR spectra of 2-phenyloxirane (styrene oxide) and 4-phenyl-1,3-dioxolan-2-one (styrene carbonate) in CDCl<sub>3</sub>.



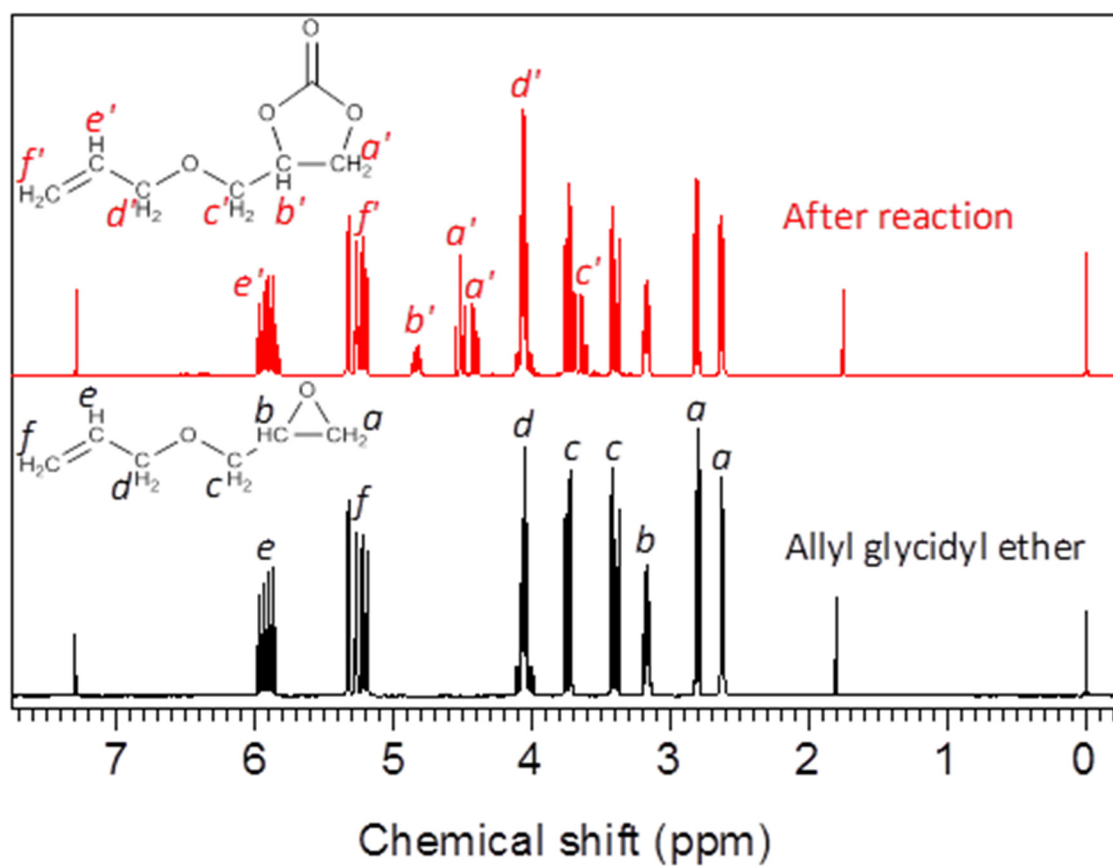


Figure S9. <sup>1</sup>H-NMR spectra of 2-(prop-2-enoxymethyl)oxirane (allyl glycidyl ether) and 4-((allyloxy)methyl)-1,3-dioxolan-2-one (allyl glycidyl carbonate) in CDCl<sub>3</sub>.

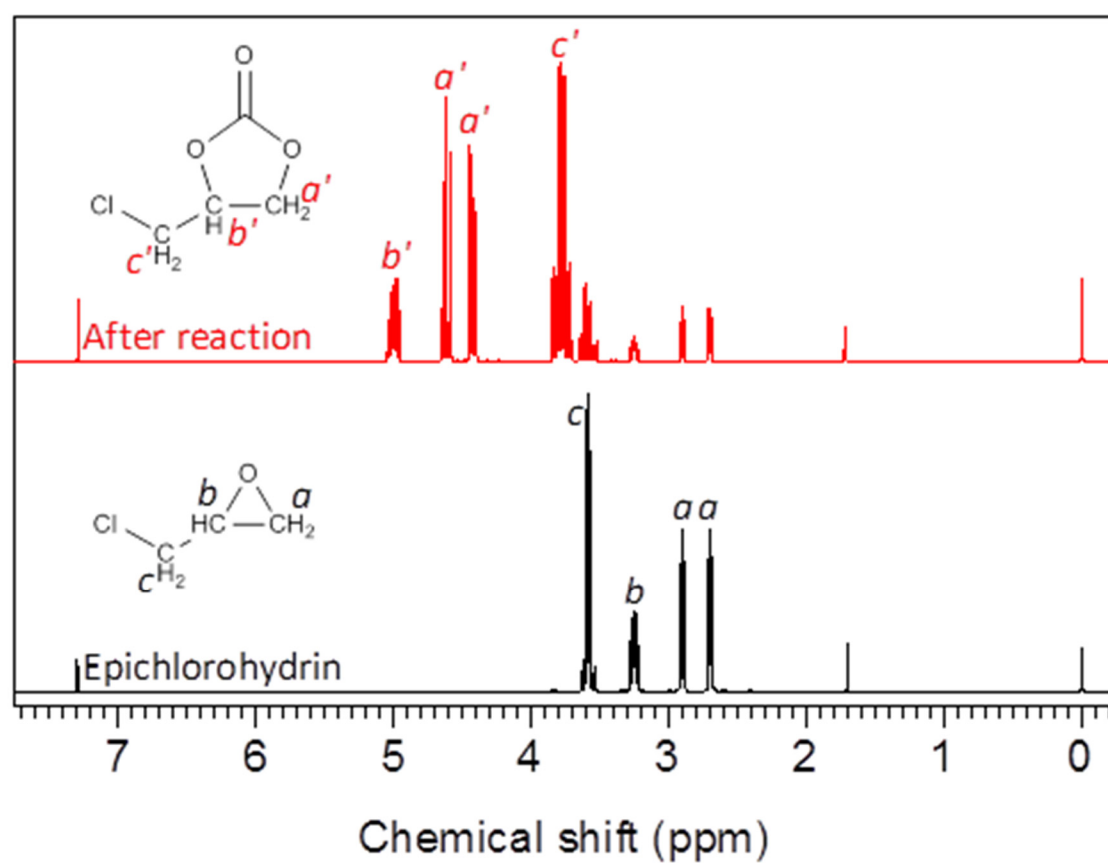


Figure S10. <sup>1</sup>H-NMR spectra of 2-(chloromethyl)oxirane (epichlorohydrin) and 4-(chloromethyl)-1,3-dioxolan-2-one (chloropropene carbonate) in CDCl<sub>3</sub>.

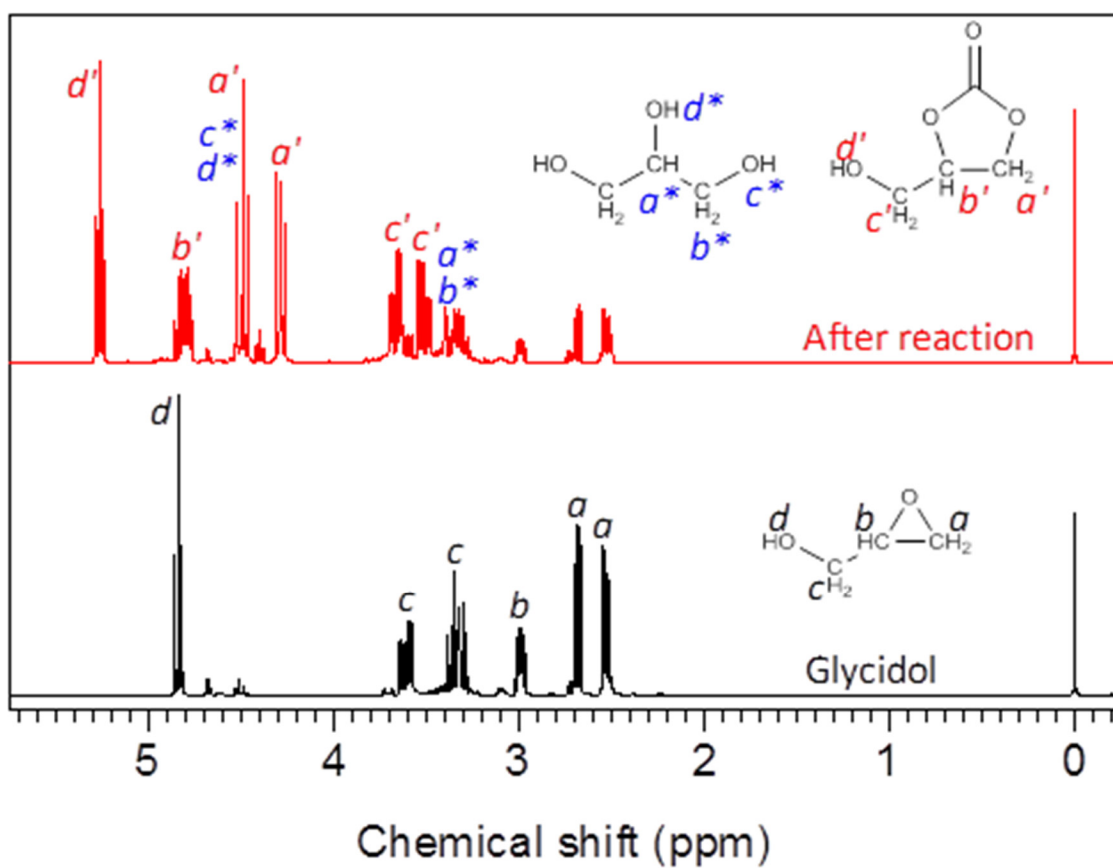


Figure S11.  $^1\text{H}$ -NMR spectra of oxiran-2-ylmethanol (glycidol) and 4-(hydroxymethyl)-1,3-dioxolan-2-one (glycerol carbonate) in  $\text{DMSO-d}_6$ .